Research Article | Vol. 11, No. 10 / 1 October 2020 / Biomedical Optics Express 6027
Biomedical Optics EXPRESS

In-vitro study of monocytic THP-1 leukemia cell membrane elasticity with a single-cell microfluidic-assisted optical trapping system

RIC JOHN L. OMBID,[1,2] GLENN G. OYONG,[1,4] ESPERANZA C. CABRERA,[3,4] WILFRED V. ESPULGAR,[5] MASATO SAITO,[5,6] EIICHI TAMIYA,[6,7] AND ROMERIC F. POBRE[1,2,*]

[1]*OPTICS Research Unit, CENSER, De La Salle University (DLSU), Manila, Philippines*
[2]*Optics and Instrumentation Physics Laboratory, Physics Department, DLSU, Manila, Philippines*
[3]*Biology Department, DLSU, Manila, Philippines*
[4]*Molecular Science Unit Laboratory, CENSER, DLSU, Manila, Philippines*
[5]*Department of Applied Physics, Graduate School of Engineering, Osaka University, Japan*
[6]*Advanced Photonics and Biosensing Open Innovation Laboratory, AIST-Osaka University, Photonics Center, Osaka University, Osaka 565-0871, Japan*
[7]*The Institute of Scientific and Industrial Research, Osaka University, Japan*
[*]*romeric.pobre@dlsu.edu.ph*

Abstract: We studied the elastic profile of monocytic THP-1 leukemia cells using a microfluidic-assisted optical trap. A 2-μm fused silica bead was optically trapped to mechanically dent an immobilized single THP-1 monocyte sieved on a 15-µm microfluidic capture chamber. Cells treated with Zeocin and untreated cells underwent RT-qPCR analysis to determine cell apoptosis through gene expression in relation to each cell's deformation profile. Results showed that untreated cells with 43.05 ± 6.68 Pa are more elastic compared to the treated cells with 15.81 ± 2.94 Pa. THP-1 monocyte's elastic modulus is indicative of cell apoptosis shown by upregulated genes after Zeocin treatment. This study clearly showed that the developed technique can be used to distinguish between cells undergoing apoptosis and cells not undergoing apoptosis and which may apply to the study of other cells and other cell states as well.

1. Introduction

Chemical-based staining and detection protocols include sample preparation that requires histological dyes or immunolabeling that is costly, laborious, and may affect the cell's integrity. Recently, the mechanical properties of a cell have shown promising outcomes as an alternative label-free biomarker assay that can differentiate cell state [1,2]. Moreover, studying cell's mechanical properties can provide additional information about biological processes such as adhesion, proliferation, and migration [3]. Also, cell profiling of cells using mechanical properties has been tested for fibroblast cells using a dual-optical trap [4] and holographic optical tweezers [5], and for malignant and metastatic cells using optical stretcher [6]. This was supported by the work of Kaffas et al. in 2014 that mechanical property can differentiate normal cells from cancerous cells [7]. Typical mechanical properties of a cell include elasticity, deformability, adhesiveness, viscosity, and many others. Several techniques are currently available in elucidating these mechanical properties such as atomic force microscopy (AFM) [8], magnetic twisting cytometry [9], micropipette aspiration [10,11], and optical trapping [12–15]. However, the atomic force microscopy technique uses a pointed cantilever that may damage the cells and requires dry sample preparation that cannot mimic the cell environment. Magnetic twisting cytometry and micropipette aspiration, on the other hand, are limited to larger cells. The current optical trapping technique makes use of vertical indentation to determine the mechanical properties of a cell [16].

#402526 https://doi.org/10.1364/BOE.402526
Journal © 2020 Received 13 Jul 2020; revised 20 Sep 2020; accepted 23 Sep 2020; published 1 Oct 2020

Biomedical Optics EXPRESS

However, this technique has a limited axial displacement range for the microbead handler due to the random background noise of the surrounding media arising from the Brownian motion of an aqueous solution. To address this limitation, we implemented a single-cell microfluidic-assisted optical trapping technique that uses spherical microbeads that can minimize cell damage and can accommodate wider space for cell movement. Moreover, the microfluidic platform has the advantage of holding and isolating single cells for easy location of the cells. This provides for faster elasticity moduli acquisition times suitable for a single-cell THP-1 monocyte that rapidly divides.

Cell membrane elasticity is one of the many ways to identify cytoskeletal cell alterations that has the potential of determining the treatment efficacy for terminal illnesses, such as cancer, which is one of the leading causes of death worldwide [17]. In the Philippines alone, leukemia has a five-year survival rate of 5.2% and accounts for the 4,270 new cancer cases in 2015 [18]. Some anticancer drugs inhibit the abnormal proliferation of cancer by targeting the specific pathway that will lead to apoptosis or cell death. Several studies suggest that apoptosis is associated with the upregulation of the *cfos* and *cjun* gene expressions [19–21]. The early apoptotic *cfos* and *cjun* marker genes can be activated by drugs that stimulate the cAMP pathway or Ca^{2+} elevation. Moreover, *cfos* and *cjun* are known to be associated with the cytoskeletal functions of the cell that contributes to its mechanical properties. In addition, *akt* or protein kinase B is an important regulator for cell survival, growth, and more importantly in actin reorganization [22–24]. Furthermore, actin cytoskeleton reorganization largely contributes to the mechanical properties of cells [25,26]. Thus, targeting signaling pathways that lead to the inhibition of *akt* gene expression and the induction of *cfos* and *cjun* gene expressions may have the ability to modify the mechanical properties of cells.

In this study, monocytic THP-1 leukemia cells were treated with Zeocin, an anticancer drug known to downregulate growth-promoting *akt* gene and upregulate early apoptosis-promoting *cfos* and *cjun* gene expressions cascading to cytoskeletal effects through actin filament reorganization. The expressions of these anti-apoptotic and pro-apoptotic genes were compared to the elasticity profile of THP-1 after the administration of the drug. Measurement of membrane elasticity modulus is a label-free biomarker that may not only address the high cost of medical tests, extensive procedures, and cell modification due to chemical staining but also an indicator for early apoptosis of cells—leading to the discovery of potential cancer treatments. Moreover, this study can be extended to profiling other types of cells.

2. Materials, experimental setup, and method

2.1. Cells and cell culture

The THP-1 human monocytic leukemia cell line (American Type Culture Collection, Manassas, VA, USA) was provided by the Molecular Science Unit Laboratory (MSUL), Center for Natural Science and Environmental Research (CENSER), De La Salle University, Manila. THP-1 cells were maintained and cultured following standard protocol in a complete medium composed of Dulbecco's Modified Eagle's Medium (DMEM, Invitrogen, USA), 10% fetal bovine serum (FBS), and 1x antibiotic-antimycotic. Growth was attained at 37°C in a humidified incubator supplemented with 5% CO_2 until 90% confluence prior to harvesting. The cells were then harvested, and an aliquot was stained with trypan blue to determine viable cell counts under a hemocytometer.

2.2. Microfluidic device fabrication

The fabrication materials and equipment for the microfluidic chip was provided by Nanobio Engineering group at Osaka University, Japan. The fabrication consisted of two parts – the master mold (silicon wafer) lithography printing and the microfluidic chip (PDMS polymer) following the

Biomedical Optics EXPRESS

protocol of Lake *et al*. [27]. Initially, the diameter of THP-1 cells (n = 90, ø = 13.02 ± 2.15 µm) was measured using a DS-Fi3-L4 microscope (Nikon Corporation) to estimate the capture chamber. The microfluidic chip was designed using AutoCAD2019 (Autodesk Inc.). Subsequently, a master mold (4-inch silicon wafer) was coated with SU-8 negative photoresist (SU-8 3025, MicroChem Corp., Westborough, MA, USA). It was then exposed to ultraviolet light using the maskless lithography machine (NanoSystems Solutions, Inc.) following the design of the microfluidic platform. The UV-exposed molecules crosslinked to form the structure, while the unexposed molecules remained soluble and were removed using SU-8 developer (MicroChem Corp., Westborough, MA, USA). Afterward, metal eyelets were glued at the inlet and outlet of the channel to support the silicon tubes. The polydimethylsiloxane (PDMS) was mixed containing the PDMS base and curing agent (Silpot 184, Dow Corning Toray, Tokyo, Japan) with a 10:1 ratio. PDMS was chosen because it has a transparent, low auto-fluorescence, and biocompatible properties. The fabricated PDMS microfluidic chip has a thickness of 1.5 mm and has 468 trapping sites with 0.015 mm width, 0.010 mm length, and 0.025 mm height. The PDMS microfluidic chip was bonded to a micro cover glass slide with 50 × 70 × 0.1 mm (Matsunami Glass Ind, Ltd.) using a plasma surface treatment (PDC210, Yamato Scientific Co., Ltd.).

2.3. Cytotoxic treatment with Zeocin

A total of 100 µL aliquots containing 1×10^5 viable THP-1 cells per mL in complete DMEM were seeded into each well of a 96-well plate and incubated overnight in a humidified incubator at 37°C supplemented with 5% CO_2. The cells were then exposed to two-fold serial dilutions of Zeocin at 100, 50, 25, 12.5, 6.25, 3.123, 1.56, and 0.78 µg/mL concentrations followed by further incubation for 24 hours. Wells with untreated cells served as the negative control. Ten µL of PrestoBlue viability reagent (Invitrogen, USA) was added into each well and incubated for a minimum of 4 hours at 37°C with 5% CO_2 in a humidified chamber to allow the remaining viable cells to metabolically convert blue resazurin to red resorufin. Spectrophotometric measurements were performed at 570 nm (BioTek Instruments, USA) to obtain optical density readings from which cytotoxicity indexes (CI%) were calculated using Eq. (1) below:

$$\text{CI\%} = 100 - \left(\frac{OD_{570}\ treated}{OD_{570}\ untreated} \right) 100 \tag{1}$$

where OD_{570} is the measured optical density at 570 nm. The CI% values of Zeocin were used to determine the optimum concentration that resulted in a 50% cell viability reduction (IC_{50}). The IC_{50} value was extrapolated from dose-response curves via nonlinear regression analysis using GraphPad Prism v.7.01 (GraphPad Software, Inc., USA). The calculated IC_{50} value was used as the concentration for the treatment of THP-1 cells in subsequent experiments.

2.4. Reverse transcription quantitative polymerase chain reaction (RT-qPCR) of akt, cfos, and cjun transcripts

RT-qPCR was performed according to standard methods with a few variations [28]. Firstly, a T-50 flask containing 5 mL THP-1 cells (1×10^5 viable cells per mL) were treated with the IC_{50} of Zeocin and incubated for 24 hours. A similar T-50 flask without Zeocin treatment was prepared as the untreated control. The cells were harvested and total RNA was extracted from both untreated and Zeocin-treated cells using Trizol (Invitrogen, USA) following the manufacturer's instructions. Reactions for RT-qPCR were prepared as 10 µL volumes each containing 1.0 µL RNA, 1x KAPA One-Step SYBR (Roche, Switzerland) Fast Buffer I, 1x KAPA reverse transcriptase, 0.3 µM of each primer (Table 1), and Diethyl Pyrocarbonate (DEPC)-treated water. The reactions were subjected to initial cDNA synthesis at 50 °C for 3 mins followed by the actual PCR profile consisting of 45 cycles of 95 °C for 1 min (denaturation), 55 °C for 1 min (annealing), and 72 °C for 1 min (extension). A melting curve was performed thereafter. The same reaction was

Biomedical Optics EXPRESS

independently performed using primers for *gapdH*, the endogenous housekeeping gene control. The critical cycle threshold (Ct) was obtained from the built-in Rotor Gene software (RGQ v. 2.3.1.49). From the Ct value data, the relative gene expression $2^{(-\Delta\Delta Ct)}$ of *akt, cfos*, and *cjun* genes were calculated.

Table 1. Primer sequence for the amplification of *akt, cfos, cjun*, and *gapdH* gene transcripts

Target gene	Primer sequence (5'-3')
akt	Forward: ATGAGCGACGTGGCTATTGTGAAG
	Reverse: GAGGCCGTCAGCCACAGTCTGGAT
cfos	Forward: AGGAGAATCCGAAGGGAAAGGAATAAGATGGCT
	Reverse: AGACGAAGGAAGACGTGTAAGCAGTGCAGCT
cjun	Forward: GCATGAGGAACCGCATTGCCGCCTCCAAGT
	Reverse: GCGACCAAGTCCTTCCCACTCGTGCACACT
gapdH	Forward: AGTCCTTCCACGATACCAAAGT
	Reverse: CATGAGAAGTATGACAACAGCCT

2.5. Microfluidic-assisted optical trapping

The membrane elasticity of THP-1 cells was measured using the microfluidic-assisted optical trapping (Figs. 1(a)–1(b)) that consisted of optical trapping (Impetux Optics S. L.) and microfluidic technology. The continuous-wave laser beam (Thorlabs, Compact laser Diode, $\lambda = 976$ nm) was focused using an objective lens (Nikon Plan Fluor 100x, oil) with a numerical aperture of 1.30. The sample chamber is made of a microfluidic platform (0.17 mm thick glass slide) with a working distance of 0.33 mm above the objective lens. The microfluidic platform was mounted on a piezo stage (Thorlabs, 3-Axis NanoMax Stage) that provides nanometer resolution for three-dimensional positioning of the sample. The optical trapping stiffness was calibrated using the power spectrum method with a 1μm/step position resolution.

There are two consecutive protocols in measuring the cell membrane elasticity: the optical trapping of the 2.06 μm non-functionalized silica microparticles (Bangs Laboratories) using a 976 nm laser diode with an incident power of 200 mW and the capturing of ~13 μm sized single-cell THP-1 monocytes inside a PDMS microfluidic chip. Briefly, a mixture of 2.06 μm beads and THP-1 monocyte cells were injected at the inlet of the microfluidic chip. After 3-5 minutes of cell sieving inside the microfluidic chip, the THP-1 cells occupied all the capturing sites. Afterward, the 976 nm laser was activated to trap and control the nearest bead for cell indentation with a 24.72 pN trapping force. The XYZ piezo stage where the THP-1 monocytes are captured inside the microfluidic chip moved transversely towards the optically trapped bead to deform the moving incident cell. Figures 1(c)–1(f) shows the experimental setup of the sieving of cells using a microfluidic chip and trapping of the bead using an optical tweezer.

2.6. Membrane elasticity of THP-1

The modulus of elasticity or Young's modulus was determined using the Hertz approximation model. This is a geometry dependent contact theory of two spherical surfaces considering that there are no adhesion and friction between the two materials [29]. The elasticity can be quantified by the following equation

$$E = \frac{3}{4}\frac{F}{d^{3/2}R^{1/2}} \tag{2}$$

where F is the indentation force, d is the depth, and R is the relative radii [30]. The relative radii R of the two materials are given by $1/R = 1/R_1 + 1/R_2$, which can be rewritten into

Biomedical Optics EXPRESS

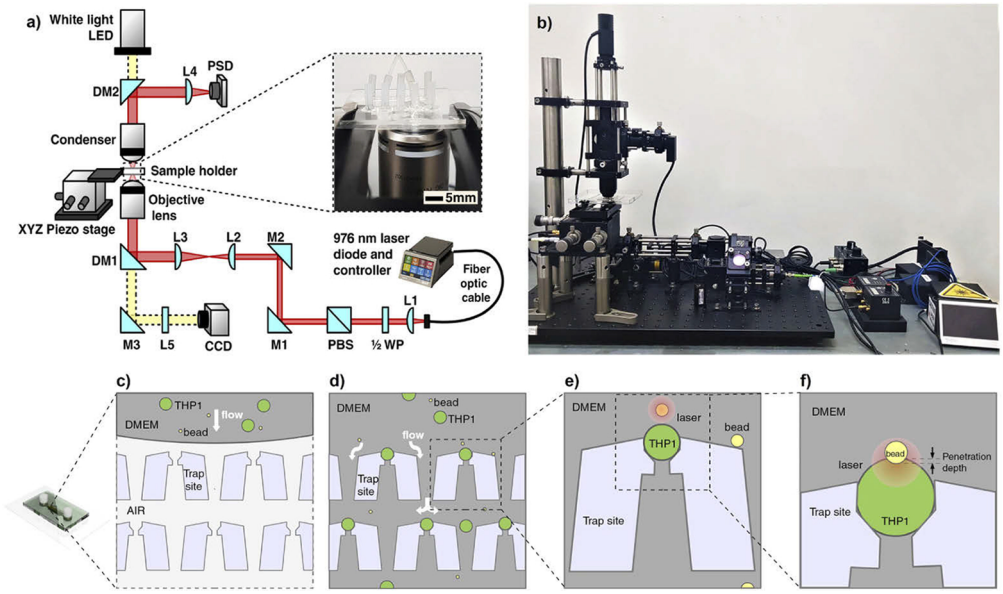

Fig. 1. a) Microfluidic-assisted optical trapping configuration; L: Lens, WP: waveplate, PBS: Polarizing beam splitter, M: mirror, DM: dichroic mirror, CCD: Charged-coupled device, PSD: Position sensitive detector. b) The actual microfluidic-assisted optical trapping setup. (c-f) Elasticity measurement of THP-1 cells. c) A mixture of THP-1 cells (**green**) and 2 µm fused silica beads (**yellow**) in DMEM is infused into the inlet which flows onto the trapping sites of the microfluidic chip. d) THP-1 cells are captured inside the trap site. e) The 976 nm laser (**red**) is turned on at 200 mW to trap the beads. f) The piezo stage is moved towards the bead to deform the cells.

$R = (R_1R_2)/(R_1 + R_2)$. For two different elastic objects in contact, the effective elastic modulus of the system is $1/E = 1 - {v_1}^2/E_1 + 1 - {v_2}^2/E_2$, where E_n is the elastic modulus, and v_n is the Poisson's ratio. Poisson's ratio is the degree of contraction or expansion of material perpendicular to the loading direction. The subscripts 1 and 2 denote the two different materials. The elastic modulus of the fused silica bead is around 70 GPa or 7×10^5 K/cm^2, which is large compared to the cell, having the second term of effective elastic modulus will be assumed zero [31]. Thus, the elasticity of the cell E_1 becomes [32]:

$$E_1 = \frac{3}{4}\frac{(1-v^2)\,F}{d^{3/2}\,R^{1/2}}. \tag{3}$$

2.7. Statistical analysis

For the cytotoxicity and RT-qPCR experiments, all samples were assayed in triplicate. The gathered data are presented as mean ± standard error of the mean unless stated otherwise. A two-sample Students' T-test was used to determine the statistical differences between the untreated THP-1 cells and Zeocin-treated THP-1 cells. In our analysis, a p-value of <0.05 was considered statistically significant.

3. Results

3.1. Trapping capability of PDMS microfluidic chip

The design of the microfluidic chip was based on a hydrodynamic microfluidic method that has a mechanism to sort and isolate single THP-1 cells. It consists of inlet, filter, trapping sites, and

Biomedical Optics EXPRESS

outlet as shown in Fig. 2. The single-cell 69% trapping efficiency of the microfluidic chip was determined by imaging and counting the trapped cells. Several parameters affect the trapping efficiency of the microfluidic chip, but in this study, we considered the flow rate, flow guide, and flow resistance between the main channel and the trapping channel in the design. The cells were loaded at a flow rate of 0.5 ml/min.

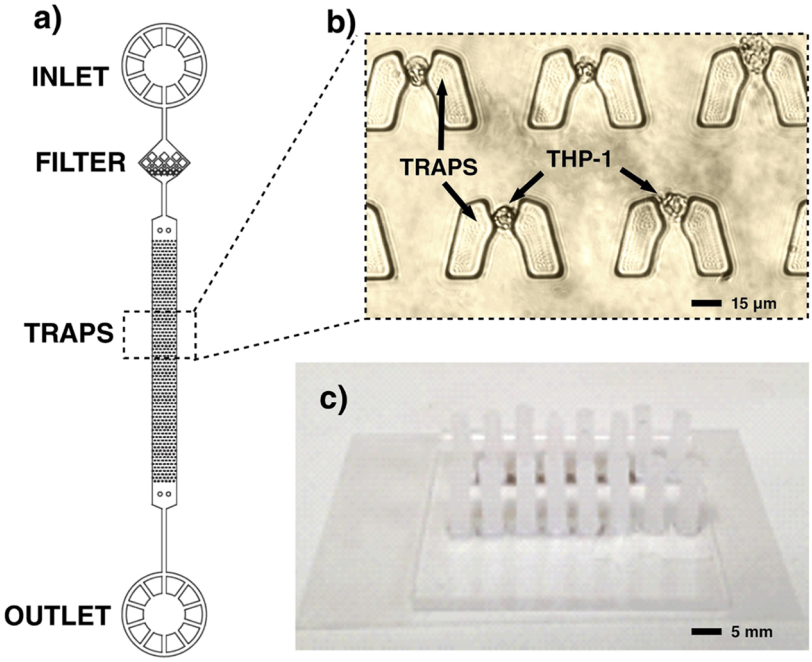

Fig. 2. Illustration showing the a) microfluidic chip parts, b) trapped THP-1 cells in a trapping site, and c) the fabricated microfluidic chip.

3.2. Cytotoxicity of Zeocin on THP-1 cells

The cytotoxicity indices (CI%) were plotted against Zeocin concentrations ($\log_{10}$). Based on the cytotoxicity index (CI%) plots via nonlinear regression (Fig. 3), the IC_{50} of the anticancer drug, Zeocin was calculated. Based on the results, Zeocin is cytotoxic to THP-1 cells with an IC_{50} value of 9.17 µg/mL. According to the American National Cancer Institute (ANCI), the accepted criteria for the cytotoxicity activity for pure compounds is 10 µg/mL [33]. The measured IC_{50} value is below the accepted standard, hence we used Zeocin for the experiment to ensure that the cells will commit early apoptosis.

3.3. Regulation of akt, cfos, and cjun gene expression

Changes in the regulation of expressions of the anti-apoptotic *akt* gene and early proapoptotic *cfos* and *cjun* genes were determined to confirm apoptosis and to associate this with changes in cell membrane elasticity. RT-qPCR results showed that the *akt*, *cfos*, and *cjun* gene expressions ($2^{-\Delta\Delta Ct}$) of THP-1 cells ($2.18 \times 10^4 \pm 2.58 \times 10^3$, 8.47 ± 2.94, and 10.58 ± 1.42, respectively) changed significantly after administration of Zeocin (7.52 ± 3.18, $4.38 \times 10^4 \pm 5.80 \times 10^3$, and $2.97 \times 10^4 \pm 1.09 \times 10^4$, respectively) as shown in Fig. 4. The relative gene expression of the anti-apoptotic *akt* gene was significantly downregulated ($p < 0.05$), while the relative gene expression of *cfos* and *cjun* genes were significantly upregulated ($p < 0.05$) compared to untreated controls.

Biomedical Optics EXPRESS

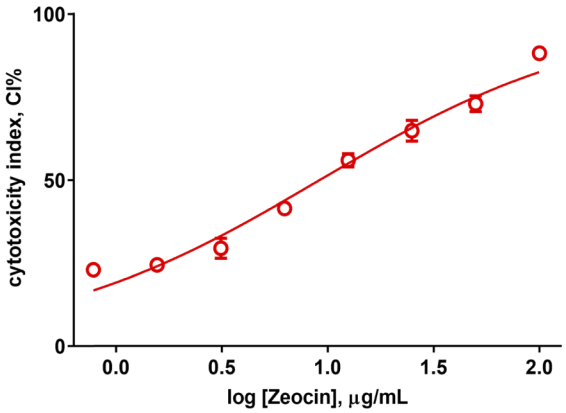

Fig. 3. Dose-response curve of THP-1 cells after treatment with two-fold serial dilutions of Zeocin.

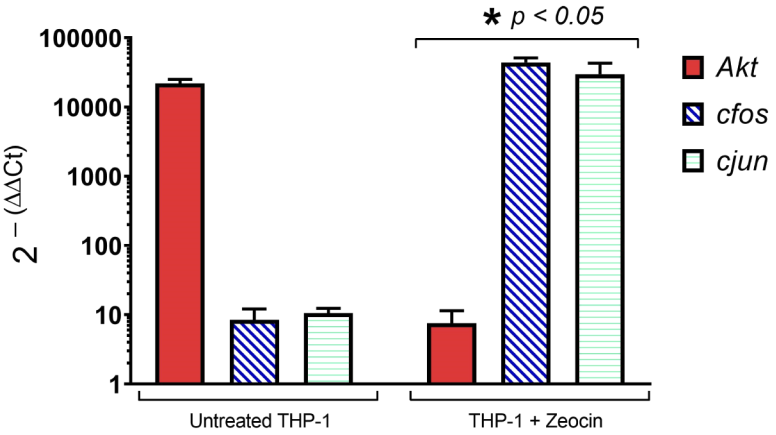

Fig. 4. Relative gene expression ($2^{-\Delta\Delta Ct}$ values) of anti-apoptotic marker *Akt* gene and early apoptotic markers *cfos* and *cjun* genes for untreated and treated THP-1 cells.

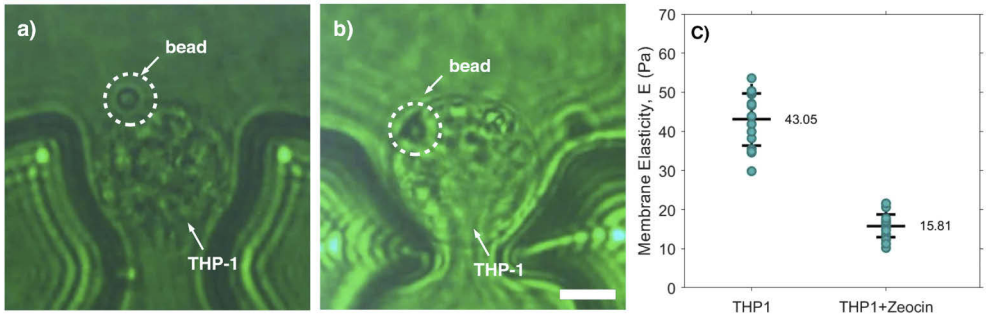

Fig. 5. Cell membrane deformation of (a) THP-1 cell and (b) THP-1 + Zeocin (scale bar = 5 µm). c) The scatter plot of membrane elasticity modulus of THP-1 compared to THP-1 with Zeocin.

Biomedical Optics EXPRESS

3.4. Alteration of the cellular membrane of THP-1 cells

To determine the effect of *akt* inhibition, and *cfos* and *cjun* increased expression, we employed microfluidic-assisted optical trapping to determine the membrane elasticity. The results showed that the membrane elasticity of THP-1 cells (43.05 ± 6.68 Pa, $n = 11$) was altered after exposure to Zeocin (15.81 ± 2.94 Pa, $n = 9$) as shown in Fig. 5. This suggests that the decrease in expressions of the *akt* gene and an increase in expressions of *cfos* and *cjun* genes of THP-1 cells resulted in a decrease in membrane elasticity ($p < 0.05$). Thus, the administration of Zeocin onto the THP-1 cells could alter its elastic moduli.

4. Discussion

The elastic modulus of a material determines the material's resistance to being deformed. The lower elastic modulus signifies that the cell can be easily deformed when force is applied. Microfluidic-assisted optical trapping was used to measure the membrane elasticity of monocytic leukemia cells treated and not treated with an anticancer agent, Zeocin. However, according to other research works, the 976 nm laser used can induce heat absorption and photodamage on cells after a long exposure, such as for greater than five minutes [34,35]. In this research, the optical tweezer trapped a highly transparent microbead that offered no direct near-IR radiation exposure and no thermal conduction on the single cell. In addition, the optical tweezer used a laser diode with a 200 mW incident power that had approximately 1 μm diffraction limited beam spot size and a 2 μm sized optically trapped microbead, where the microbead was larger than the focused beam spot. Thus, photodamage on a single cancer cell could be minimized under these optical trapping conditions.

The Zeocin-treated flask contained 99.95% non-viable cells as measured using the trypan blue assay. Counting was done 24 hours after Zeocin treatment. The relative percentage of non-viable cells was calculated by back-tracking from the transcript copy numbers in which each had a corresponding cycle threshold (Ct), and deriving the relative number of cells from the standard curve of the *gapdh* housekeeping gene assayed using known concentrations of 10^2, 10^3, 10^4, 10^5, 10^6, 10^7, and 10^8 copies/μL (7 orders of magnitude). Each concentration had a relative number of cells based on the copy number of the housekeeping gene per cell. At the same time, the Zeocin-treated cells showed the upregulation of the expression of the early apoptotic *cfos* and *cjun* genes and the downregulation of the expression of the anti-apoptotic *akt* gene. These substantiate that the THP-1 cells tested for membrane elasticity were mostly undergoing early apoptosis.

The RT-qPCR results showed that Zeocin treatment inhibited the expression of the anti-apoptotic *akt* gene and upregulated the expression of the pro-apoptotic *cfos* and *cjun* genes. The regulation of these genes is nominally an indication of the apoptosis of the cell. Moreover, it can be attributed to the alteration of actin filaments [12,36]. The actin filamentary structures are parts of the cytoskeleton that provides cell support and shape. Consequently, the disaggregation of actin filaments is always followed by a decrease in cellular membrane elasticity [37]. Other techniques have been used to investigate the alteration of mechanical properties and its relationship with actin reorganization [38,39]. The changes in the mechanical properties are associated with the activation of p38 mitogen-activated protein kinases (MAPK) pathway [38,40]. The deficiency of MAPK would lead to the cytoskeletal reorganization of the cell [41,42]. Furthermore, the activation of the MAPK signaling pathway regulates *cjun* gene expression [43,44], triggers *cfos* gene expression [44,45], and interplays with the *akt* signaling pathway [46]. Thus, the regulation of these gene expressions can be attributed to the decrease in cell membrane elasticity after the administration of Zeocin.

The current study demonstrated that the THP-1 cells undergoing apoptosis had lower elastic modulus and is highly related to the regulation of the gene expression of the *akt* (anti-apoptotic), and *cfos* and *cjun* (early pro-apoptotic) genes. The current findings are supported by the results

Biomedical Optics EXPRESS

of previous reports. The measured elasticity is within the typical elastic modulus of eukaryotic cells that ranges from 10^1 Pa to 10^3 Pa [47]. Moreover, the mechanical properties of cells may decrease or increase after the administration of drugs because of the distinct apoptotic pathways in the cell [11]. Chemotherapeutic drugs usually target the cytoskeleton of cells that will affect the stiffness or elasticity of cells [48].

Overall, this study demonstrated that the decrease in the elasticity of the cell membrane was related to the upregulation of the expression of early pro-apoptotic genes *cfos* and *cjun* and the downregulation of the expression of the pro-apoptotic gene *akt.* Interestingly, changes in membrane elasticity can provide information about the metabolic processes of the cells when exposed to anticancer drugs. Moreover, the use of the microfluidic-assisted optical trapping can be applied to other cell types, treatments of cells at varying concentrations, and treatments of cells over time.

5. Conclusion

In-vitro cell membrane elasticity analysis indicated that the THP-1 leukemia cells treated with Zeocin exhibited lower elastic modulus compared to the untreated cells. This alteration in the membrane elasticity can be attributed to the regulation of the gene expressions. Comparative gene expression analysis showed that the anti-apoptotic *akt* gene expression and pro-apoptotic *cfos* and *cjun* gene expressions in THP-1 cells were downregulated and upregulated respectively after Zeocin treatment. The reduction of membrane elasticity was largely attributed to the ongoing cell apoptosis of THP-1 leukemia cells due to Zeocin. Another technical highlight of this study is the integrated use of the microfluidic system and optical trapping system, a promising optical tool, and a novel microfluidic platform in performing elastic moduli measurements for rapidly dividing cells like THP-1 leukemia cells as a biomarker without using chemical staining to differentiate cell state.

Funding

Philippine Council for Industry, Energy, and Emerging Technology Research and Development (04125).

Acknowledgment

The authors wish to extend their sincerest gratitude to Prof. Eiichi Tamiya from Nanobio-engineering Laboratory of Osaka University, Japan for the fabrication of the microfluidic chip.

Disclosures

The authors declare no conflicts of interest.

References

1. X. Su, L. Zhang, H. Kang, B. Zhang, G. Bao, and J. Wang, "Mechanical, nanomorphological and biological reconstruction of early stage apoptosis in HeLa cells induced by cytochalasin-B," Oncol. Rep. (2018).
2. F.-S. Quan and K. S. Kim, "Medical applications of the intrinsic mechanical properties of single cells," Acta Biochim. Biophys. Sin. **48**(10), 865–871 (2016).
3. L. Andolfi, E. Bourkoula, E. Migliorini, A. Palma, A. Pucer, M. Skrap, G. Scoles, A. P. Beltrami, D. Cesselli, and M. Lazzarino, "Investigation of Adhesion and Mechanical Properties of Human Glioma Cells by Single Cell Force Spectroscopy and Atomic Force Microscopy," PLoS One **9**(11), e112582 (2014).
4. F. Schlosser, F. Rehfeldt, and C. F. Schmidt, "Force fluctuations in three-dimensional suspended fibroblasts," Philos. Trans. R. Soc., B **370**(1661), 20140028 (2015).
5. S. Fusco, P. Memmolo, L. Miccio, F. Merola, M. Mugnano, A. Paciello, P. Ferraro, and P. A. Netti, "Nanomechanics of a fibroblast suspended using point-like anchors reveal cytoskeleton formation," RSC Adv., **6**(29), 24245–24249 (2016).

Biomedical Optics EXPRESS

6. J. Guck, S. Schinkinger, B. Lincoln, F. Wottawah, S. Ebert, M. Romeyke, D. Lenz, H. M. Erickson, R. Ananthakrishnan, D. Mitchell, J. Kas, S. Ulvick, and C. Bilby, "Optical deformability as an inherent cell marker for testing malignant transformation and metastatic competence," Biophys. J.**88**(5), 3689–3698 (2005).
7. A. E. Kaffas, D. Bekah, M. Rui, J. C. Kumaradas, and M. C. Kolios, "Investigating longitudinal changes in the mechanical properties of MCF-7 cells exposed to paclitaxol using particle tracking microrheology," Phys. Med. Biol. **58**(4)), 923–936 (2013).
8. J. A. Hessler, A. Budor, K. Putchakayala, A. Mecke, D. Rieger, M. M. B. Holl, B. G. Orr, A. Bielinska, J. Beals, and J. Baker, "Atomic Force Microscopy Study of Early Morphological Changes during Apoptosis," Langmuir **21**(20)), 9280–9286 (2005).
9. N. Wang and D. Ingber, "Control of cytoskeletal mechanics by extracellular matrix, cell shape, and mechanical tension," Biophys. J. **66**(6), 2181–2189 (1994).
10. R. M. Hochmuth, "Micropipette aspiration of living cells," J. Biomech **33**(1), 15–22 (2000).
11. S. Vigmostad, B. Krog, J. Nauseef, M. Henry, and V. Keshav, "Alterations in cancer cell mechanical properties after fluid shear stress exposure: a micropipette aspiration study," *Cell Health and Cytoskeleton*, 25 (2015).
12. M. Unal, Y. Alapan, H. Jia, A. G. Varga, K. Angelino, M. Aslan, and U. A. Gurkan, "Micro and Nano-Scale Technologies for Cell Mechanics," Nanobiomedicine **1**, 5 (2014).
13. H. Wu, J. Zhu, Y. Huang, D. Wu, and J. Sun, "Microfluidic-Based Single-Cell Study: Current Status and Future Perspective," Molecules **23**(9), 2347 (2018).
14. F. Basoli, S. M. Giannitelli, M. Gori, P. Mozetic, A. Bonfanti, M. Trombetta, and A. Rainer, "Biomechanical Characterization at the Cell Scale: Present and Prospects," Frontiers in Physiology **9**, 1449 (2018).
15. S. Khakshour, M. P. Labrecque, H. Esmaeilsabzali, F. J. S. Lee, M. E. Cox, E. J. Park, and T. V. Beischlag, "Retinoblastoma protein (Rb) links hypoxia to altered mechanical properties in cancer cells as measured by an optical tweezer," Sci. Rep. **7**(1), 7833 (2017).
16. M. S. Yousafzai, "Cancer cell mechanics and cell microenvironment: an optical tweezers study", Ph.D. thesis, University of Trieste (2015).
17. K. Fraczkowska, M. Bacia, M. Przybyło, D. Drabik, A. Kaczorowska, J. Rybka, E. Stefanko, S. Drobczynski, J. Masajada, H. Podbielska, T. Wrobel, and M. Kopaczynska, "Alterations of biomechanics in cancer and normal cells induced by doxorubicin," Biomed. Pharmacother. **97**, 1195–1203 (2018).
18. A. V. Laudico, M. R. Mirasol-Lumague, V. Medina, F. G. Valenzuela, and E. Pukkala, "2015 Philippine cancer facts and estimates," Jul-2017. [Online]. Available: http://www.philcancer.org.ph/wp-content/uploads/2017/07/2015-PCS-Ca-Facts-Estimates_CAN090516.pdf.
19. J. Galea, "Alterations in c-fos expression, cell proliferation and apoptosis in pressure distended human saphenous vein," Cardiovasc. Res. **44**(2), 436–448 (1999).
20. R. G. Syljuåsen, J.-H. Hong, W. H. Mcbride, and R. G. Syljuasen, "Apoptosis and Delayed Expression of c-jun and c-fos after Gamma Irradiation of Jurkat T Cells," Radiat. Res. **146**(3)), 276 (1996).
21. T. Oshitari, M. Dezawa, S. Okada, M. Takano, H. Negishi, H. Horie, H. Sawada, T. Tokuhisa, and E. Adachi-Usami, "The role of c-fos in cell death and regeneration of retinal ganglion cells," Investigative Ophthalmology and Visual Science **43**(7), 2442–2449 (2002).
22. A. Enomoto, H. Murakami, N. Asai, N. Morone, T. Watanabe, K. Kawai, Y. Murakumo, J. Usukura, K. Kaibuchi, and M. Takahashi, "Akt/PKB regulates actin organization and cell motility via girdin/APE," Dev. Cell **9**(3), 389–402 (2005).
23. G. Xue and B. A. Hemmings, "PKB/akt-dependent regulation of cell motility," J. Natl. Cancer Inst. **105**(6), 393–404 (2013).
24. Z. Fan, C. Li, C. Qin, L. Xie, X. Wang, Z. Gao, Wang Qiangbacuozhen, T. Yu, and L. H. Liu, "Role of the PI3 K/AKT pathway in modulating cytoskeleton rearrangements and phenotype switching in rat pulmonary arterial vascular smooth muscle cells," DNA Cell Biol., **33**(1), 12–19. (2014)
25. I. Jalilian, C. Heu, H. Cheng, H. Freittag, M. Desouza, J. R. Stehn, N. S. Bryce, R. M. Whan, E. C. Hardeman, T. Fath, G. Schevzov, and P. W. Gunning, "Cell elasticity is regulated by the tropomyosin isoform composition of the actin cytoskeleton," PLoS One **10**(5), e0126214–23 (2015).
26. Y. M. Efremov, A. A. Dokrunova, A. V. Efremenko, M. P. Kirpichnikov, K. V. Shaitan, and O. S Sokolova, "Distinct impact of targeted actin cytoskeleton reorganization on mechanical properties of normal and malignant cells," Biochim. Biophys. Acta, Mol. Cell Res. **1853**(11), 3117–3125 (2015).
27. M. Lake, M. Lake, C. Narciso, K. Cowdrick, T. Storey, S. Zhang, J. Zartman, and D. Hoelzle, "Microfluidic device design, fabrication, and testing protocols," Protocol Exchange July 1–26 (2015).
28. P. T. Shyu, G. G. Oyong, and E. C. Cabrera "Cytotoxicity of Probiotics from Philippine Commercial Dairy Products on Cancer Cells and the Effect on Expression of cfos and cjun Early Apoptotic-Promoting Genes and Interleukin-1 β and Tumor Necrosis Factor- α Proinflammatory Cytokine Genes. (L)." (2014).
29. K. K. Liu, D. R. Williams, and B. J. Briscoe, "The large deformation of a single micro-elastomeric sphere," J. Phys. D: Appl. Phys. **31**(3), 294–303 (1998).
30. K. L. Johnson, *Contact Mechanics* (Cambridge University Press, 1985).
31. A. G. Romashin and Y. E. Pivinskii, "Properties of fused silica ceramics," Refractories **9**(9-10), 590–595 (1968).
32. P. Kollmannsberger and B. Fabry, "Linear and Nonlinear Rheology of Living Cells," Annu. Rev. Mater. Res. **41**(1)), 75–97 (2011).

Biomedical Optics EXPRESS

33. M. Suffness and JM. Pezzuto, "Assays related to cancer drug discovery," In *Methods in Plant Biochemistry: Assays for Bioactivity*; K Hostettmann, Ed., Volume 6 (Academic Press, 1991) pp. 71–133.
34. B. del Rosal, P. Haro-González, W. T. Ramsay, L. M. Maestro, K. Santacruz-Gómez, M. C. la Cruz Iglesias-de, F. Sanz-Rodríguez, J. Y. Chooi, P. Rodríguez-Sevilla, D. Choudhury, A. K. Kar, J. García Solé, L. Paterson, and D. Jaque, "Heat in optical tweezers," *Optical Trapping and Optical Micromanipulation X*, **8810**, 88102A, (2013).
35. P. Haro-González, W. T. Ramsay, L. M. Maestro, B. Del Rosal, K. Santacruz-Gomez, M. D. C. La Cruz Iglesias-De, F. Sanz-Rodríguez, J. Y. Chooi, P. R. Sevilla, M. Bettinelli, D. Choudhury, A. K. Kar, J. G. Solé, D. Jaque, and L. Paterson, "Quantum dot-based thermal spectroscopy and imaging of optically trapped microspheres and single cells," Small, **9**(12), 2162–2170 (2013).
36. T. Tsakiridis, A. Bergman, R. Somwar, C. Taha, K. Aktories, T. F. Cruz, A. Klip, and G. P. Downey, "Actin Filaments Facilitate Insulin Activation of the Src and Collagen Homologous/Mitogen-activated Protein Kinase Pathway Leading to DNA Synthesis and c-fos Expression," J. Biol. Chem. **273**(43)), 28322–28331 (1998).
37. C. Rotsch and M. Radmacher, "Drug-Induced Changes of Cytoskeletal Structure and Mechanics in Fibroblasts: An Atomic Force Microscopy Study," Biophys. J. **78**(1)), 520–535 (2000).
38. S. S. An, C. M. Pennella, A. Gonnabathula, J. Chen, N. Wang, M. Gaestel, P. M. Hassoun, J. J. Fredberg, and U. S. Kayyali, "Hypoxia alters biophysical properties of endothelial cells via p38 MAPK- and Rho kinase-dependent pathways," Am. J. Physiol. Cell Physiol. **289**(3), C521–C530 (2005).
39. J. Wang, Z. Wan, W. Liu, L. Li, L. Ren, X. Wang, P. Sun, L. Ren, H. Zhao, Q. Tu, Z. Zhang, N. Song, and L. Zhang, "Atomic force microscope study of tumor cell membranes following treatment with anti-cancer drugs," Biosens. Bioelectron. **25**(4), 721–727 (2009).
40. L. Hoffman, C. C. Jensen, M. Yoshigi, and M. Beckerle, "Mechanical signals activate p38 MAPK pathway-dependent reinforcement of actin via mechanosensitive HspB1," Mol. Biol. Cell **28**(20), 2661–2675 (2017).
41. D. O'Malley and J. Harvey, "MAPK-dependent actin cytoskeletal reorganization underlies BK channel activation by insulin," EJONEI **25**(3), 673–682 (2007).
42. A. M. Tormos, S. Rius-Pérez, M. Jorques, P. Rada, L. Ramirez, Á. M. Valverde, Á. R. Nebreda, J. Sastre, and R. Taléns-Visconti, "P38α regulates actin cytoskeleton and cytokinesis in hepatocytes during development and aging," PLoS One **12**(2), e0171738–22 (2017).
43. M. Kayahara, X. Wang, and C. Tournier, "Selective Regulation of c-jun Gene Expression by Mitogen-Activated Protein Kinases via the 12- OTetradecanoylphorbol-13-Acetate- Responsive Element and Myocyte Enhancer Factor 2 Binding Sites," Mol. Cell. Biol. **25**(9), 3784–3792 (2005).
44. W. Shi, X. Hou, X. Li, H. Peng, M. Shi, Q. Jiang, X. Liu, Y. Ji, Y. Yao, C. He, and X. Lei, "Differential gene expressions of the MAPK signaling pathway in enterovirus 71-infected rhabdomyosarcoma cells," Braz. J. Infect. Dis. **17**(4), 410–417 (2013).
45. Y. Wang and R. Prywes, "Activation of the c-fos enhancer by the Erk MAP kinase pathway through two sequence elements: The c-fos AP-1 and p62(TCF) sites," Oncogene **19**(11), 1379–1385 (2000).
46. E. R. Lee, J. Y. Kim, Y. J. Kang, J. Y. Ahn, J. H. Kim, B. W. Kim, H. Y. Choi, M. Y. Jeong, and S. G Cho, "Interplay between PI3 K/Akt and MAPK signaling pathways in DNA-damaging drug-induced apoptosis," Biochim. Biophys. Acta, Mol. Cell Res. **1763**(9), 958–968 (2006).
47. E. Moeendarbary and A. R. Harris, "Cell mechanics: principles, practices, and prospects. Wiley Interdisciplinary Reviews," Wiley Interdiscip. Rev.: Syst. Biol. Med. **6**(5), 371–388 (2014).
48. H. Yu, C. Y. Tay, W. S. Leong, S. C. W. Tan, K. Liao, and L. P. Tan, "Mechanical behavior of human mesenchymal stem cells during adipogenic and osteogenic differentiation," Biochem. Biophys. Res. Commun. **393**(1), 150–155 (2010).